SANGAM International Journal of Multidisciplinary Research

Vol. 03, Issue 02, March (2026) E-ISSN: 2584-086X

Dual-Band, Dual-Polarized Two-Element Circular Slots MIMO Antenna for 5G Communication Device

Rabiu Sharif Auwal[1]* and Jitendra Vaswani[2]

[*1]Department of Electronic and Communication Engineering, Mewar University, Chittorgarh, Rajasthan, India.

[2]Department of Electronic and Communication Engineering, Mewar University, Chittorgarh, Rajasthan, India.

Corresponding Author:

Available online at: www.sijmr.org

Abstract— In this research paper, a two-element circular slot dual-band, dual-polarized MIMO antenna with circular slots is simulated and simulated for application in fifth-generation (5G) mobile communications and WLAN user equipment. The two operational frequencies are mutually independent and fall within the sub-6 GHz range, centered at frequency bands of 3.6 GHz and 5.5 GHz respectively. The source elements are mounted towards the substrate determines the antenna polarizations. To confirm its affordability, accessibility, and convenience of usage, FR-4 substrate is employed for design. The antenna set's radiation pattern is bidirectional and has good bandwidth, gain, and efficiency.

Keywords*— WLAN, MIMO, 5G, Dual-polarization, Dual-band, Sub-6 GHz*

I. INTRODUCTION

In the early years of the twenty-first century, mobile phones were primarily designed for voice communication, and internet connectivity was only considered an additional feature. During this time, the world was gradually shifting from an offline environment toward an online ecosystem. Access to the internet was largely dependent on desktop computers and laptops connected through plug-in devices, wireless adapters, or local area networks (LAN). However, during the second decade of the century, a significant transformation occurred as a majority of services and applications migrated to online platforms. Simultaneously, advancements in mobile communication technologies, particularly the evolution from 2G to 3G and subsequently to 4G networks, led to substantial improvements in data transmission speeds. These advancements increased data rates from a few kilobits per second to several megabits per second, enabling mobile devices to perform tasks far beyond simple voice communication.

With these technological improvements, smartphones became capable of supporting a wide range of applications, including high-definition video calls, live streaming of events, and numerous internet-based services. Around the same period, the concept of the Internet of Things (IoT) gained momentum. IoT allows various electronic devices and sensors to communicate with each other through the internet, enabling remote monitoring and control of connected systems. The successful implementation of such technologies requires reliable, high-speed internet connectivity while maintaining mobility for users and devices.

Although fourth-generation (4G) communication systems currently provide high-speed mobile internet services, research and development activities have been focused on the development of fifth-generation (5G) communication technology to achieve even higher data speeds and improved network performance (Vaswani & Agarwal, 2021). Today, 5G technology is gradually being adopted worldwide and is already operational in several countries such as South Korea, the United States, China, Japan, and India. One of the defining features of 5G communication is its ability to operate across two primary spectrum ranges: the millimeter-wave band and the Sub-6 GHz frequency band (Chakraborty et al., 2024). Among these, the Sub-6 GHz spectrum is often preferred during the initial deployment of 5G networks because it requires relatively fewer hardware modifications and allows easier integration with existing communication infrastructure. Furthermore, a variety of frequency bands within the Sub-6 GHz range can be utilized to support different 5G applications.

In the design of smartphone antennas, it is crucial to develop multi-band and multi-standard antenna systems that can support multiple communication technologies while maintaining high radiation efficiency and a low specific absorption rate (SAR). Researchers have also highlighted the importance of considering smartphone dimensions and structural constraints when designing antennas for mobile devices (Huo et al., 2017). In one study, a multi-band dual-polarized antenna capable of supporting communication standards from 2G to 5G was proposed for indoor mobile base station applications (Alieldin et al., 2018).

Another research effort presented an eight-port multiple-input multiple-output (MIMO) antenna system designed

for 5G communication. This system operates within the frequency range of 3.3 GHz to 4.2 GHz and achieves an isolation level greater than −14.4 dB, with antenna gain values varying between 3 dBi and 5 dBi depending on the operating frequency (Zhao et al., 2019). Similarly, a smartphone antenna configuration suitable for devices with approximately a five-inch display was introduced, consisting of eight loop antennas mounted on an FR-4 substrate. The antennas were arranged into two groups containing five and three elements, respectively. The envelope correlation coefficient (ECC) between any pair of antennas was reported to be below 0.2, while the radiation efficiency was around 40% and the gain was approximately 2 dB (Rao & Tsai, 2018).

To accommodate future smartphone designs, another study proposed a metal-frame based MIMO antenna system that integrates eight antennas within the device structure. This system supports the 3.4–3.8 GHz frequency range for 5G communication as well as the 2.496–2.69 GHz band for LTE services. Experimental results demonstrated good radiation efficiency exceeding 44% and low ECC values below 0.2 (Y. Li et al., 2018). In another work, a twelve-antenna array featuring triple-polarization characteristics was developed for operation between 3.4 GHz and 3.6 GHz. The researchers improved isolation between the antenna elements by utilizing mutually perpendicular polarization techniques (M.-Y. Li, Ban, et al., 2017).

Further advancements include the design of a planar dual-band four-element MIMO antenna intended for 5G mobile communication. This antenna employs folded single-pole radiating elements with extended L-shaped ground stubs positioned around each element. Due to multiple resonant modes, the antenna provides dual-band coverage ranging from 1.6 GHz to 3.6 GHz and from 4.1 GHz to 6.1 GHz. The SAR values were also found to remain within acceptable safety limits, making the antenna suitable for smartphone applications (Duan et al., 2019).

In another study, researchers introduced a high-isolation eight-antenna MIMO array operating around the 3.5 GHz band. The design utilized a balanced open-slot antenna structure that significantly improved isolation between adjacent antenna ports. In addition, polarization diversity was incorporated to further reduce mutual coupling between the antenna elements. The impact of human hand proximity on antenna performance was also investigated using hand phantom models (Y. Li et al., 2019).

Another proposed configuration included an eight-port antenna array with elements placed at the corners of the smartphone mainboard. The design employed orthogonally polarized square-loop radiators, which helped enhance port isolation and reduce correlation between antennas (M.-Y. Li, Xu, et al., 2017). Researchers have also discussed several design guidelines for antennas used in 5G smartphones. These include considerations such as higher screen-to-body ratios, larger battery sizes, improved antenna isolation, higher radiation efficiency, lower ECC values, and the ability to maintain performance regardless of whether the phone is held vertically or horizontally. Compatibility with existing 2G and 4G communication systems is also considered an important requirement (H.-C. Huang, 2018; Hong, 2017).

In another design approach, a previously developed self-isolated antenna structure was modified by incorporating vertical stubs to reduce the overall antenna size (Zhao & Ren, 2018). Additionally, an antenna capable of supporting up to thirteen frequency bands covering communication standards from 2G to 5G, as well as WLAN technology, was proposed for metal-frame smartphone structures. The study also examined the influence of the human hand on antenna performance (D. Huang et al., 2019).

A report published by Ericsson highlighted the advantages of integrating 5G New Radio (NR) technology with existing LTE networks. This integration can provide a cost-effective and scalable approach for improving network performance while enabling the delivery of advanced 5G services to users (A. T. E. Sites, pp. 1–12). In another study, a four-element MIMO antenna design based on split-ring resonator (SRR) loaded slot-loops was proposed to achieve multi-band operation within the 3–4 GHz frequency range for 5G communication systems (Sarkar & Srivastava, 2018). Furthermore, a dual-band dual-polarized slot antenna consisting of two radiating elements was proposed to support the 3.6 GHz band for 5G mobile communication and the 5.5 GHz band for WLAN applications (Vaswani & Agarwal, 2021).

Based on the previously discussed studies, various MIMO antenna configurations have been developed using different numbers of antenna elements. Most of the reported designs employ between two and eight antenna ports to achieve the desired performance. In this work, a dual-band and dual-polarized antenna configuration consisting of two circular slot antennas is proposed. The design supports the 3.6 GHz frequency band for 5G mobile communication as well as the 5.5 GHz band for WLAN applications. A critical aspect of multi-band antenna design is maintaining the independence of each operating frequency. In the proposed structure, a parasitic patch is placed between the feeding elements, and the antenna elements are physically separated to improve isolation between them. The proposed design also demonstrates satisfactory gain and radiation efficiency, making it a promising candidate for integration into future 5G smartphone devices.

II. ANTENNA DESIGN

The 30 mm by 30 mm antenna was developed with two circular slots and two feed lines. The antenna's resonance frequency is contingent upon the circular slot's circumference. The wavelength of the dielectric for the first resonance frequency coincides to the circumference of the outer ring $\pi*(a+b)/2$, and the second resonance frequency corresponds to the circumference of the outer ring to $\pi*(c+d)/2$. Slot (s) width is optimized to 0.375. To accomplish the required resonance frequencies at 3.6GHz and 5.5GHz, the ground structure's circular slots were constructed and optimized. The optimized variables for the

fundamental design of this antenna are displayed in the table 1 below. As seen in the transparent view of the antenna, a straight parasitic patch is positioned in this design slantingly between two feed lines on the top layer of the antenna as depicted in Figure 1 and Figure 2. Every antenna has a linear polarization and is positioned perpendicular to the others. The antenna system became dual-polarized as a result of the antenna feed arrangement. In Figure 3, the backside view of the proposed antenna is also displayed.

TABLE 1. *DESIGN PARAMETERS WITH THEIR VALUES*

Parameter	Description	Value (mm)
A	Outer diameter of the external slot	17.6
B	Inner diameter of the external slot	16.85
C	Outer diameter of the internal slot	11.78
D	Inner diameter of the internal slot	11.03
H	Height of the substrate	1.6
Lf	Length for the feed lines	11.4
Li	Length of the patch	11
t	Thickness of copper	0.035
s	Width for the slot	0.375
Wf	Width for the feed lines	3
Wi	Width of the patch	0.5
Ws	Length of the substrate	30

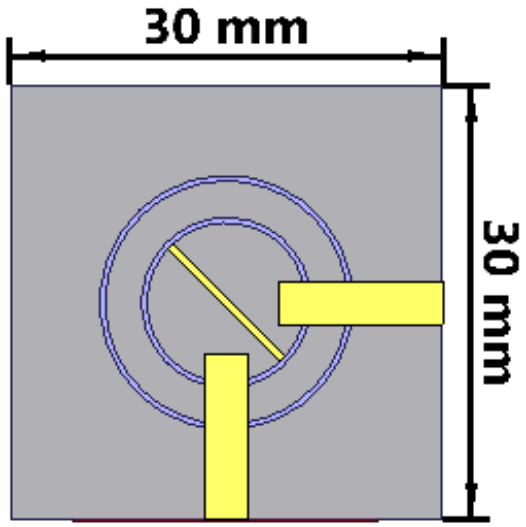

Fig. 1. The transparent view of proposed antenna

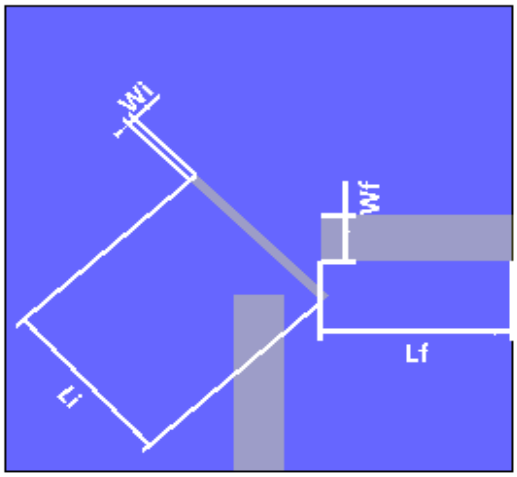

Fig.2. The front view of the antenna

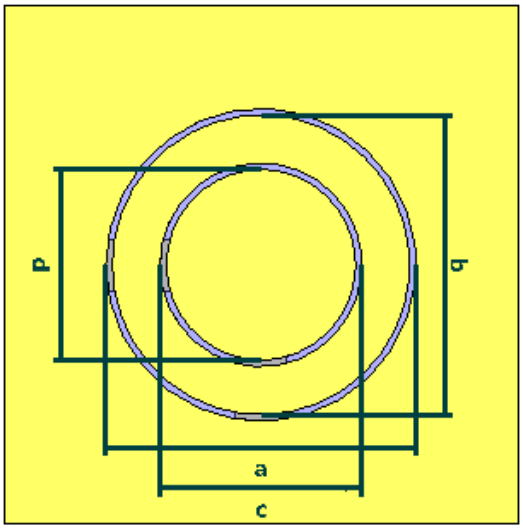

Fig.3. The back view of the proposed antenna

III. RESULTS AND DISCUSSION

Figure 4 displays the antenna's S-Parameter results. Due to the similar positioning of port 1 and port 2, this antenna resonates at the frequency bands of 3.6 GHz and 5.5 GHz, and their S-Parameters are likewise identical. The antenna's 6dB bandwidth is 490 MHz (3.36–3.85) within the lower band and 560 GHz (5.27–5.83) within the higher band. More than 17 dB of isolation is present in 3.6 GHz band, while more than 11 dB is present in 5.5 GHz range. Above 11B isolation is also caused by feed lines oriented perpendicularly due to the presence of diagonal patch. For mobile antennas, a return loss above 6 dB is regarded acceptable, and a threshold of 10 dB value is taken into consideration for isolation. The frequency bandwidth also is computed for the same levels.

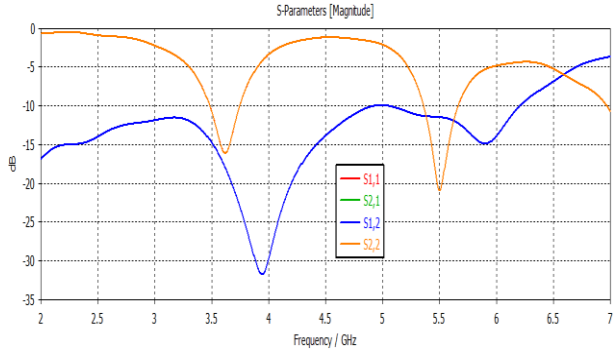

Fig. 4. S-parameter results for proposed antenna for port 1 and port 2

It was confirmed that an inverse relationship exists between the resonant frequency and the slot circumference—that is, as the slot diameter increases, the resonant frequency falls and vice versa. With the chance in the circular slots dimensions, both resonant frequencies are fluctuating separately. Figure 5 and figure 6 below illustrate the variation effects of external slot circumference 'a' and internal slot circumference 'c'.

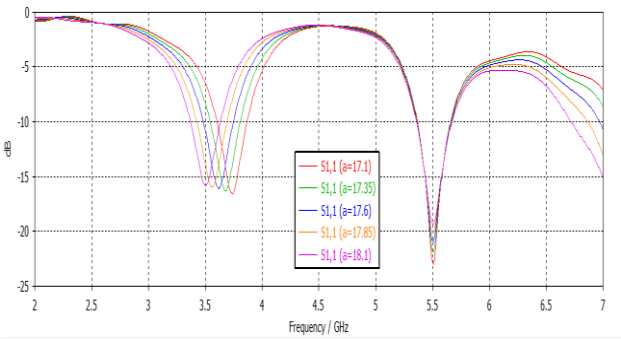

Fig. 5. The variation effect of internal slot circumference 'a'

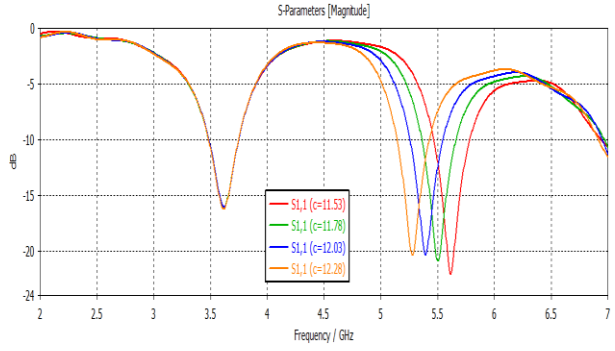

Fig. 6. The variation effect of external slot circumference 'c'

Due to the proximity of both antenna pieces, there is mutual interaction between them, especially in the 5.5GHz band, as seen in the Figures 8 to 11. A patch rectangular in shape is diagonally positioned between the two feeds-lines in order to lower the mutual coupling. Figure 7 below displays the S-parameter curves without the parasitic patch.

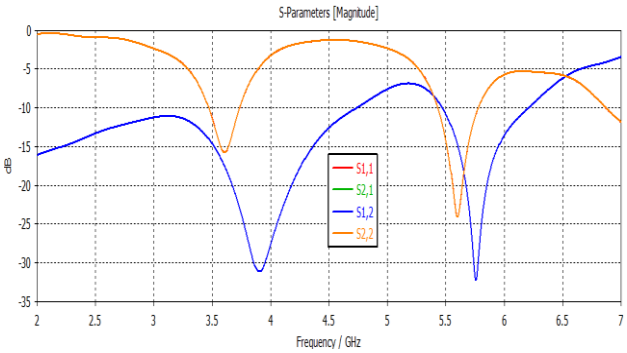

Fig. 7. S-parameter results for proposed antenna for ports 1 and 2 without parasitic patch

Figure 8 and Figure 9 for port 1 and Figure 10 and Figure 11 for port 2 correspondingly display the antenna's current distribution. The outer slot is radiating at 3.6GHz frequency in Figures 8 and 10, as can be seen by looking at the hue above the outer slot. The internal slot is also radiating at 5.5GHz frequency in Figures 9 and 11.

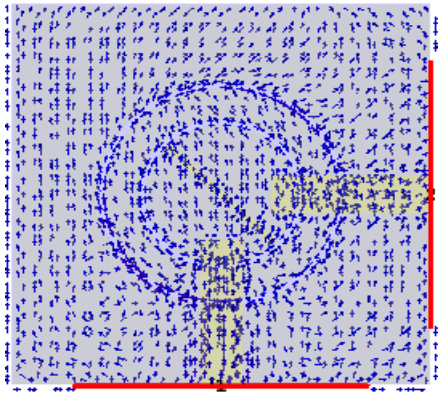

Fig. 8. Current Distribution at 3.6GHz for port 1

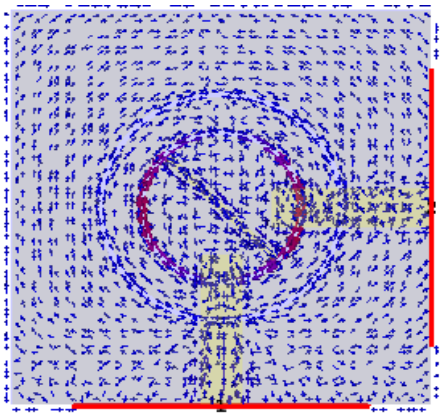

Fig.9. The Current Distribution at 5.5GHz for port 1

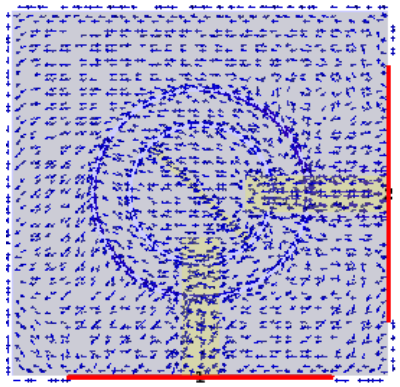

Fig. 10. Current Distribution at 3.6GHz for port 2

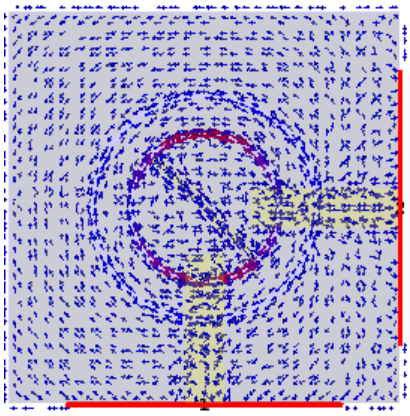

Fig.11. Current Distribution at 5.5GHz for port 2

Figures 12 and 14 illustrate the three-dimensional (3D) radiation patterns corresponding to Port 1 at operating frequencies of 3.6 GHz and 5.5 GHz, respectively. The radiation characteristics at these two frequencies exhibit similar pattern shapes. The maximum realized gain obtained is approximately 3.79 dBi at 3.6 GHz and 4.72 dBi at 5.5 GHz. Furthermore, the radiation behavior and gain performance are observed to be nearly identical for both antenna ports at the respective operating frequencies.

Figures 13 and 15 present the corresponding polar plots of the antenna gain at 3.6 GHz and 5.5 GHz. These plots provide a clearer representation of the directional radiation characteristics of the antenna at the two operating frequency bands.

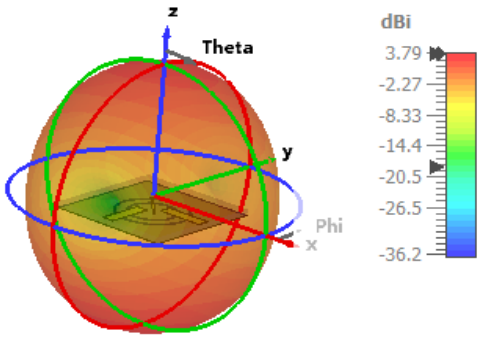

Fig.12. The 3D radiation pattern for port 1 at 3.6 GHz frequency band

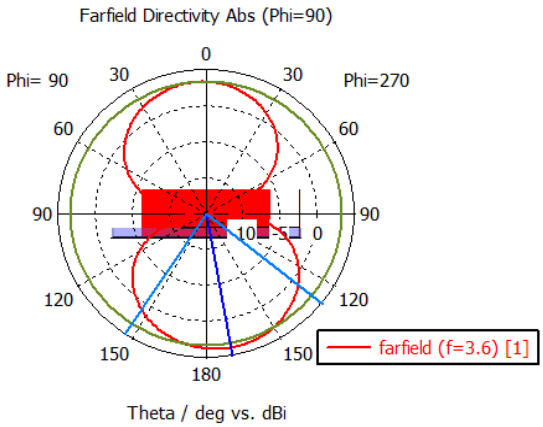

Fig.13. The polar plot of antenna radiation pattern for port 1 at frequency of 3.6 GHz

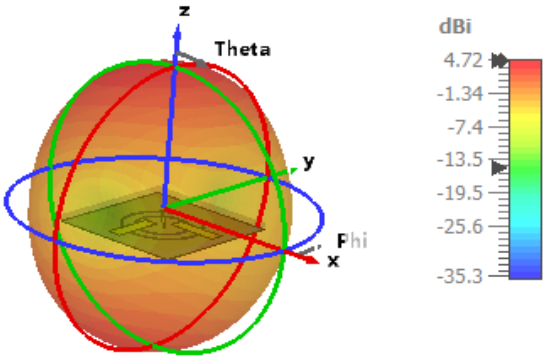

Fig.14. The 3D radiation pattern for port 1 at 5.5 GHz

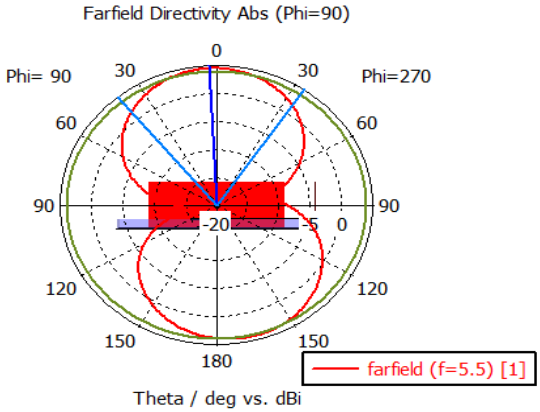

Fig.15. The polar plot of antenna at 5.5 GHz

The figure 16 below shows the radiation efficiency for the proposed antenna for ports 1 and 2. The value of more than 65% was observed for both operating ports.

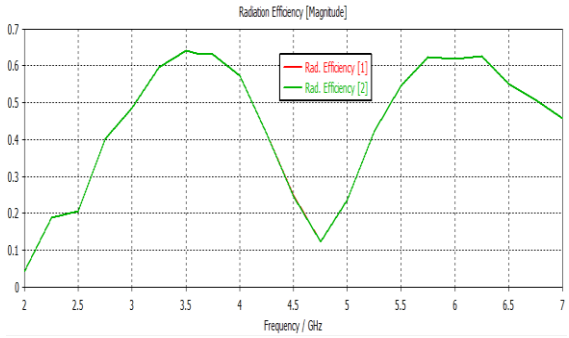

Fig.16. The radiation efficiency for the antenna for both ports 1 and 2

Since the proposed antenna is designed to operate as a multiple-input multiple-output (MIMO) system, important performance parameters such as the Envelope Correlation Coefficient (ECC) and Diversity Gain (DG) are evaluated. These parameters are calculated from the S-parameters using a post-processing technique. Figures 17 and 18 present the variation of ECC and diversity gain with respect to frequency for Port 1 and Port 2 of the antenna system.

The results indicate that within the operating frequency bands of 3.6 GHz and 5.5 GHz, the diversity gain remains close to 10, which demonstrates effective diversity performance of the MIMO system. Additionally, the ECC value stays below 0.09 across the operating range, indicating very low correlation between the antenna elements and confirming good isolation and efficient MIMO operation.

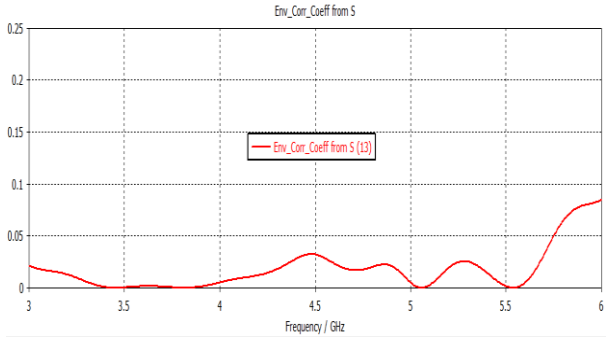

Fig.17. An envelope Correlation Coefficient (ECC) for ports 1 and 2

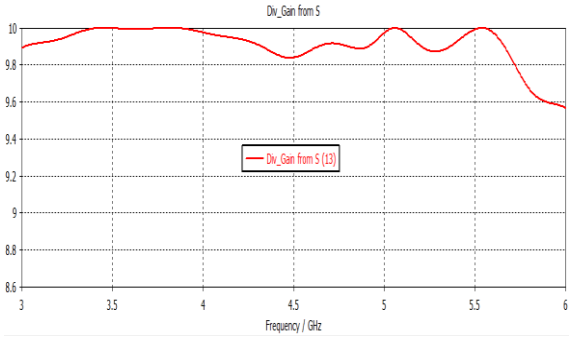

Fig.18. The diversity gain for ports 1 and 2

IV. Conclusion

This work presents a dual-band, dual-polarized two-element circular slot MIMO antenna for 5G user equipment that has dual polarization properties. The antenna has efficient, efficiency, gain, bandwidth, and enough isolation. The two operational frequency bands, 3.6 GHz and 5.5 GHz, are apart from one another. The antenna's polarization is contingent upon the orientation of the feed elements relative to the substrate. The antenna is simulated upon FR-4 substrate to guarantee both cost effectiveness and convenient availability. Consequently, the antenna has a bidirectional radiation pattern with a excellent Diversity Gain always more than 9.8 and low ECC always below 0.1.

V. Acknowledgement

I wish to express my profound gratitude to Mr. Ritesh Kumar Ojha, and Ms. Komal Yadav, for the support, and motivation throughout the course work.

I would like also to extend my thankfulness to my brother, Nuhu Sharif Auwal, and the rest members of my family for their support and belief in my abilities

References

[1] Alieldin, A., Huang, Y., Boyes, S., Stanley, M., David Joseph, S., Hua, Q., & Lei, D. (2018). A Triple-Band Dual-Polarized Indoor Base Station Antenna for 2G, 3G, 4G and Sub-6 GHz 5G Applications. *IEEE Access*, *PP*, 1–1. https://doi.org/10.1109/ACCESS.2018.2868414

[2] Chakraborty, S., Rahman, M. A., Hossain, Md. A., Nishiyama, E., & Toyoda, I. (2024). A novel dual-band elliptical ring slot MIMO antenna with orthogonal circular polarization for 5G applications. *Heliyon*, *10*(13), e33176. https://doi.org/10.1016/j.heliyon.2024.e33176

[3] Duan, J., Kuiwen, X., Li, X., Chen, S., Zhao, P., & Wang, G. (2019). Dual-band and enhanced-isolation MIMO antenna with L-shaped meta-rim extended ground stubs for 5G mobile handsets. *International Journal of RF and Microwave Computer-Aided Engineering*, *29*, e21776. https://doi.org/10.1002/mmce.21776

[4] Hong, W. (2017). Solving the 5G Mobile Antenna Puzzle: Assessing Future Directions for the 5G Mobile Antenna Paradigm Shift. *IEEE Microwave Magazine*, *18*, 86–102. https://doi.org/10.1109/MMM.2017.2740538

[5] Huang, D., Du, Z., & Wang, Y. (2019). Compact thirteen-band antenna for 4G/5G/WLAN metal frame mobile phones. *International Journal of RF and Microwave Computer-Aided Engineering*, *30*. https://doi.org/10.1002/mmce.22057

[6] Huang, H.-C. (2018). *Overview of antenna designs and considerations in 5G cellular phones* (p. 4). https://doi.org/10.1109/IWAT.2018.8379253

[7] Huo, Y., Dong, X., & Xu, W. (2017). 5G Cellular User Equipment: From Theory to Practical Hardware Design. *IEEE Access*, *5*, 13992–14010. https://doi.org/10.1109/ACCESS.2017.2727550

[8] Li, M.-Y., Ban, Y.-L., Xu, Z., Guo, J., & Z.F., Y. (2017). Tri-Polarized 12-Antenna MIMO Array for Future 5G Smartphone Applications. *IEEE Access*, *PP*, 1–1. https://doi.org/10.1109/ACCESS.2017.2781705

[9] Li, M.-Y., Xu, Z., Ban, Y.-L., Sim, C.-Y.-D., & Z.F., Y. (2017). Eight-port Orthogonally Dual-Polarized MIMO Antennas Using Loop Structures for 5G Smartphone. *IET Microwaves, Antennas & Propagation*, *11*. https://doi.org/10.1049/iet-map.2017.0230

[10] Li, Y., Sim, C.-Y.-D., Luo, Y., & Yang, G. (2018). Metal-frame-integrated eight-element multiple-input multiple-output antenna array in the long term evolution bands 41/42/43 for fifth generation smartphones. *International Journal of RF and Microwave Computer-Aided Engineering*, *29*, e21495. https://doi.org/10.1002/mmce.21495

[11] Li, Y., Sim, C.-Y.-D., Luo, Y., & Yang, G. (2019). High-Isolation 3.5-GHz 8-Antenna MIMO Array Using Balanced Open Slot Antenna Element for 5G Smartphones. *IEEE Transactions on Antennas and Propagation*, *PP*, 1–1. https://doi.org/10.1109/TAP.2019.2902751

[12] Rao, L.-Y., & Tsai, C.-J. (2018). *8-Loop Antenna Array in the 5 Inches Size Smartphone for 5G Communication the 3.4 GHz-3.6 GHz Band MIMO Operation* (p. 1999). https://doi.org/10.23919/PIERS.2018.8598072

[13] Sarkar, D., & Srivastava, K. V. (2018). *Four Element Dual-band Sub-6 GHz 5G MIMO Antenna Using SRR-loaded Slot-Loops*. https://doi.org/10.1109/UPCON.2018.8596789

[14] Vaswani, J., & Agarwal, A. (2021). Dual-Band, Dual-Polarized Two Element Slot Antenna for Fifth Generation Mobile Devices. *Turkish Journal of Computer and Mathematics Education (TURCOMAT)*, *12*(3), 4822–4830. https://doi.org/10.17762/turcomat.v12i3.1986

[15] Zhao, A., & Ren, Z. (2018). Size Reduction of Self-Isolated MIMO Antenna System for 5G Mobile Phone Applications. *IEEE Antennas and Wireless Propagation Letters*, *PP*, 1–1. https://doi.org/10.1109/LAWP.2018.2883428

[16] Zhao, A., Ren, Z., & Wu, S. (2019). Broadband MIMO Antenna System for 5G Operations in Mobile Phones. *International Journal of RF and Microwave Computer-Aided Engineering*, *29*. https://doi.org/10.1002/mmce.21857

